第 32 卷第 10 期
2015 年 10 月

控 制 理 论 与 应 用
Control Theory & Applications

Vol. 32 No. 10
Oct. 2015

DOI: 10.7641/CTA.2015.50406

小型四旋翼无人机双闭环轨迹跟踪与控制

许　璟, 蔡晨晓†, 李勇奇, 邹　云

(南京理工大学 自动化学院, 江苏 南京 210094)

摘要: 近年来, 无人飞行器控制繁荣发展对控制精度与品质要求日益增高. 为了应对这一挑战, 本文基于奇异摄动的思想设计了四旋翼无人机非线性轨迹跟踪控制器. 首先, 基于牛顿欧拉定律建立了四旋翼无人飞行器非线性奇异摄动形式的数学模型. 然后, 引入奇异摄动理论, 通过时间尺度分解的方法将系统解耦成内环快子系统和外环慢子系统. 再者, 根据非线性动态逆的思想分别建立快、慢伪线性子系统, 并基于此分别设计外环轨迹跟踪、内环稳定子控制器, 综合子控制器生成应用于原系统的全阶控制器以兼顾跟踪精度和鲁棒特性. 针对内环快系统, 采用线性二次调节控制器以实现稳定快速地控制飞行器旋转动态; 针对外环慢系统, 运用经典的比例–微分–积分控制器以跟踪所给定的轨迹. 最后给出了仿真实例说明本文结论的有效性.

关键词: 无人飞行器; 仿真器; 非线性控制; 奇异摄动思想; 比例–微分–积分控制器; 线性二次调节控制器

中图分类号: TP273　　**文献标识码**: A

Dual-loop path tracking and control for quad-rotor miniature unmanned aerial vehicles

XU Jing, CAI Chen-xiao†, LI Yong-qi, ZOU Yun

(School of Automation, Nanjing University of Science and Technology, Nanjing Jiangsu 210094, China)

Abstract: The recent development of unmanned aerial vehicle flight control creates a strong demand for higher control accuracy and control quality. To meet such demands, we propose a nonlinear control strategy for path tracking control of quad-rotor miniature unmanned aerial vehicles (MAVs). Firstly, based on Newton-Euler's laws, the nonlinear mathematical model of a quad-rotor MAV is built in singular perturbation form. By singular perturbation theory and time-scaling techniques, we decouple the system into the fast inner-loop sub-system and the slow outer-loop subsystem. Then, we build the fast pseudo-linear sub-system and the slow pseudo-linear sub-system based on the nonlinear dynamic inversion idea. On the basis of these subsystems, we respectively design the outer sub-controller for path tracking and the inner sub-controller for stabilization. These two sub-controllers are combined into a full-order controller for the original system to achieve the required tracking accuracy and robustness. In the fast inner sub-system, we use the LQG controller to realize the rapid control for the rotary dynamics of the aerial vehicle; in the slow outer sub-system, we employ the classical PID controller to track the given path. Simulation results show the effectiveness of the conclusions made in this paper.

Key words: unmanned aerial vehicles; simulators; nonlinear control; singular perturbation; proportional integral derivative control; linear quadratic regular control

1 Introduction

Recent advances in the investigation of unmanned vehicles have led to enormous exciting developments, particularly, with the platform of quad-rotor miniature unmanned aerial vehicles (MAVs). As opposed to fixed wing vehicles, the quad-rotor MAV is a smal-scale vehicle which might be more suitable for specific applications including search and rescue, surveillance and remote inspection. The ability to maneuver an actual MAV accurately along a given geometric path is a primary objective for most applications. Previous work on path tracking of MAVs has concentrated on techniques such as feedback linearization, sliding mode control, proportional integral derivative control (PID) control, linear quadratic regular (LQR) control and backstepping control methods [1–9]. In [1], a global trajectory tracking control of UAVs without linear velocity measurements was designed based on inverse dynamic approaches. The authors in [2] proposed a backstepping design for the trajectory tracking problem of a class of underactuated systems where the states are guaranteed to con-

Received 15 May 2015; accepted 11 July 2015.

†Corresponding author. E-mail: ccx5281@vip.163.com.

Supported by the Fundamental Research Funds for the Central Universities (30920140112005, 30915011105, 30915011104).

verge to a ball near the origin. A continuous sliding mode control method based on feedback linearization was presented in [3], and an output tracking control was designed for a quad-rotor UAV. As demonstrated in [4], a classical PID controller made a quad-rotor able to track a given reference trajectory in presence of minor perturbations.

On the other hand, singular perturbations and time-scale techniques (SPaTSs) have been proven to be effective tools for model reduction, analysis and design of flight control systems. Modeling both kinematics and dynamics of quad-rotor MAVs results in a model with high order, which may decrease feasibility of controller design. The main concept of SPaTSs is to lower the model order by neglecting the fast part, and to improve the the approximation by reintroducing their effects as boundary layer corrections in separate time-scales [10]. In [11], the design and stability analysis of a hierarchical controller via using SPaTSs was presented. Flight test trajectory control systems based on time-scale techniques were designed to enable the pilot to follow complex trajectories for evaluating an aircraft within its known flight envelop and to explore the boundaries of its capabilities [12]. A cascade decomposition method was discussed in [13] for the longitudinal dynamics of a low-speed experimental UAV.

In this paper, we present a strategy of path tracking for a quad-rotor MAV to reduce position errors, and to follow a reference geometric path. Based on SPaTSs, models for inner- and outer-loops have been constructed in different time-scales. The inner-loop controller is made by integration of dynamic inversion approaches and LQR control method to enhance stability, and the two time-scale characteristics can be preserved to facilitate controller design. The outer-loop controller combines a dynamic inversion controller with a PID controller to ensure a desired tracking performance. The dual-loop control structure is adopted to coordinate inner-loop and outer-loop controls, which can simplify the design procedure, and improve control quality and quantity of the flight system. The main contribution of this paper is outlined as follows:

1) Different from current works, the mathematical model of a quad-rotor MAV in this paper is represented in the singular perturbed, affine nonlinear form to facilitate controller design.

2) The dual loop control structure is then utilized to facilitate decomposition, and to attenuate the controller design difficulty of under-actuated MAVs. In this sense, inner-loop and outer-loop controller design can be done separately in different time-scales.

3) Input control energy is saved under the assumption that small position errors are permitted. It should be noted that the position of a MAV is guaranteed within a pipe centered on the given path.

4) Due to wind effects, there exists large initial position errors off the references. The control strategy of this work can eliminate the initial errors quickly, and enable the MAV track the reference path within a specified precision.

5) The modeling/control approach in this paper delivers controllers that exploit both translational and orientational dynamic capability of the aircraft, and thus are ready to be used by higher level navigation systems for complex autonomous missions.

Notation Throughout this paper, I_n is the $n\times n$ identity matrix of order n. $\mathbb{R}^n$ and $\mathbb{R}^{n\times m}$ denote, respectively, the n-dimensional Euclidean space and the set of all $n\times m$ real matrices. The superscripts "T", "$*$", "$\dagger$" denote matrix transposition, complex transpose and the Moore-Penrose inverse. The $s_{\rm x}$ and $c_{\rm x}$ notations represent $\sin x$ and $\cos x$ respectively. Matrices, if not explicitly stated, are assumed to have compatible dimensions.

2 Dynamic modeling of the quad-rotor UAV

A quad-rotor MAV is controlled by the rotational speeds of four rotors. The Newton-Euler formulation is adopted to develop the mathematical model of the quad-rotor UAV. The vehicle is represented using a right hand Inertial coordinate system (I) of axes and a right hand body frame (B). From [14], the equations of motion can take the concrete form in the body frame (see also in Table 1),

$$\begin{cases} \dot{u} = -(wq - vr) - {\rm g}s\theta, \\ \dot{v} = -(ur - wp) + {\rm g}c\theta s\phi, \\ \dot{w} = -(vp - uq) + {\rm g}c\theta s\theta + u_1/m, \\ \dot{\phi} = p + qs\phi\tan\theta + rc\phi\tan\theta, \\ \dot{\theta} = qc\phi - rs\phi, \\ \dot{\psi} = qs\phi\sec\theta + rc\phi\sec\theta, \\ \dot{p} = (I_{\rm y} - I_{\rm z})/I_{\rm x}qr + u_2/I_{\rm x}, \\ \dot{q} = (I_{\rm z} - I_{\rm x})/I_{\rm y}pr + u_3/I_{\rm y}, \\ \dot{r} = (I_{\rm x} - I_{\rm y})/I_{\rm z}pq + u_4/I_{\rm z}, \end{cases} \tag{1}$$

where

$$\begin{cases} u_1 = F_1 + F_2 + F_3 + F_4, \\ u_2 = (-F_2 + F_4)l, \\ u_3 = (-F_1 + F_3)l, \\ u_4 = (-F_1 + F_2 - F_3 + F_4)\lambda, \end{cases} \tag{2}$$

in which l is the distance between the motor and the center of mass, λ is the scaling factor from the force to moment and m is the body total mass of UAV.

Table 1 Formulation notations

Notations	Description	Unit
$(u,\ v,\ w)$	Translational velocities	m/s
$(p,\ q,\ r)$	Rotational velocities	rad/s
$(\phi,\ \theta,\ \psi)$	Euler angles (roll, pitch, yaw)	rad
$(I_{\rm x},\ I_{\rm y},\ I_{\rm z})$	Rotational inertias	kg· m^2

Taking the rotation matrix

$$R(\Theta)=\begin{bmatrix} c\theta c\psi & s\phi s\theta c\psi - c\phi s\psi & c\phi s\theta c\psi + s\phi s\psi \\ c\theta s\psi & s\phi s\theta s\psi + c\phi c\psi & c\phi s\theta s\psi - s\phi c\psi \\ -s\theta & s\phi c\theta & c\phi c\theta \end{bmatrix},$$

the position vector in the inertial reference frame ($\mathcal{I}$) can be calculated by

$$\begin{cases} \dot{x} = c\theta c\psi u + (s\phi s\theta c\psi - c\phi s\psi)v + \\ \qquad (c\phi s\theta c\psi + s\phi s\psi)w, \\ \dot{y} = c\theta s\psi u + (s\phi s\theta s\psi + c\phi c\psi)v + \\ \qquad (c\phi s\theta s\psi - s\phi c\psi)w, \\ \dot{z} = -s\theta u + s\phi c\theta v + c\phi c\theta w. \end{cases} \tag{3}$$

Considering the fact that the closed-loop angular rates evolve faster than the remaining dynamics, S-PaTSs have been proven to be effective tools to simplify the high-order UAV model (1). Denoting the slow and fast variables as

$$x = [u\ \ v\ \ w\ \ \phi\ \ \theta\ \ \psi]^{\rm T},\ \ z = [p\ \ q\ \ r]^{\rm T},$$

the singularly perturbed form of (1) is derived,

$$\begin{cases} \dot{x} = f(x)z + u_{\rm s}, \\ \epsilon\dot{z} = g(z) + u_{\rm f}, \end{cases} \tag{4}$$

where

$$f(x)=\begin{bmatrix} 0 & w & -v & 1 & s\phi\tan\theta & 0 \\ -w & 0 & u & 0 & c\phi & s\phi\sec\theta \\ v & -u & 0 & c\phi\tan\theta & -s\phi & c\phi\sec\theta \end{bmatrix}^{\rm T},$$

$$u_{\rm s} = [0\ \ 0\ \ u_1/m\ \ 0\ \ 0\ \ 0]^{\rm T},$$

$$g(z) = \begin{bmatrix} (I_{\rm y}-I_{\rm z})/I_{\rm x}\epsilon qr \\ (I_{\rm z}-I_{\rm x})/I_{\rm y}\epsilon pr \\ (I_{\rm x}-I_{\rm y})/I_{\rm z}\epsilon pq \end{bmatrix},\ \ u_{\rm f} = \begin{bmatrix} 1/I_{\rm x}\epsilon u_2 \\ 1/I_{\rm y}\epsilon u_3 \\ 1/I_{\rm z}\epsilon u_4 \end{bmatrix},$$

and ϵ is a positive parameter to characterize two time-scale nature of the UAV flight control system. Considering the nonlinear nature of functions $f(x)$ and $g(z)$, the classical slow-fast decomposition approach fails to work because it is difficult to get the unique solution of z as $z_{\rm s} = h(t, x, u_{\rm f})$ for order reduction. To make up for this drawback, the fast variable z can be selected as the pseudo control input of x due to the relationship $0 = g(z_{\rm s}) + u_{\rm fs}$, as $\epsilon \to 0$, where $z_{\rm s}$ is the quasi-steady state of z.

Then, the slow subsystem (outer-loop model), $\Sigma_{\rm out}$, can be obtained,

$$\dot{x} = \bar{f}(x)\bar{u}_{\rm s}, \tag{5}$$

where $\bar{f}(x) = [f(x)\ \ I]$, $\bar{u}_{\rm s} = [z_{\rm s}\ \ u_{\rm s}]^{\rm T}$. The only fast variables $z_{\rm f}$ can be defined as

$$z_{\rm f} = z - z_{\rm s},\ \ u_{\rm ff} = u_{\rm f} - u_{\rm fs},$$

and we can obtain the reduced fast subsystem (inner-loop model), $\Sigma_{\rm in}$, as

$$\epsilon\dot{z}_{\rm f} = (g(z_{\rm f} + z_{\rm s}) - g(z_{\rm s})) + u_{\rm ff}, \tag{6}$$

rewritten in the fast time-scale $\tau = t/\epsilon$ as

$$\frac{{\rm d}z_{\rm f}}{{\rm d}\tau} = (g(z_{\rm f} + z_{\rm s}) - g(z_{\rm s})) + u_{\rm ff}. \tag{7}$$

It should be pointed out that $z_{\rm s}$ and $u_{\rm fs}$ can be regarded as constants in the fast time-scale.

3 Analysis and controller design

The trajectory tracking controller, applied directly to the flight control system, consists of inner- and outer-loop controllers. The inner-loop controller provides high stabilization of the vehicle's angular velocity by combing dynamic inversion approaches with LQR control techniques. The PID control strategy, along with direct measurements of the linear velocity, angular velocity and position from Inertial Measurement Unit, is utilized in the decouple outer-loops to achieve desired tracking performance. In this case, the slow components of angular velocities are selected as pseudo controls of the outer-loops to solve the control design difficulty caused by the under-actuated nature of the vehicle. For the path tracking applications, time-scale separation between inner and outer-loops is sufficient to guarantee that the interacted terms can be ignored during the controller design procedure. In the sequel, we focus on the controller design for subsystems $\Sigma_{\rm in}$ and $\Sigma_{\rm out}$.

3.1 Inner-loop controller design

As mentioned, the slow variable $z_{\rm s} = [\bar{p}\ \ \bar{q}\ \ \bar{r}]^{\rm T}$ can be treated as constants in the fast time-scale τ. The inner-loop model can be represented in detail as

$$\begin{cases} \dot{p}_{\rm f} = a_2(q_{\rm f}r_{\rm f} + \bar{q}r_{\rm f} + q_{\rm f}\bar{r}) + b_2u_{2\rm f}, \\ \dot{q}_{\rm f} = a_3(p_{\rm f}r_{\rm f} + \bar{p}r_{\rm f} + p_{\rm f}\bar{r}) + b_3u_{3\rm f}, \\ \dot{r}_{\rm f} = a_4(p_{\rm f}q_{\rm f} + \bar{p}q_{\rm f} + p_{\rm f}\bar{q}) + b_4u_{4\rm f}, \end{cases} \tag{8}$$

where

$$a_2 = (I_{\rm y} - I_{\rm z})/I_{\rm x}\epsilon,\ a_3 = (I_{\rm z} - I_{\rm x})/I_{\rm y}\epsilon,$$
$$a_4 = (I_{\rm x} - I_{\rm y})/I_{\rm z}\epsilon,\ b_2 = \epsilon/I_{\rm x},\ b_3 = \epsilon/I_{\rm y},$$
$$b_4 = \epsilon/I_{\rm z},\ u_{\rm ff} = [b_2u_{2\rm f}\ \ b_3u_{3\rm f}\ \ b_4u_{4\rm f}]^{\rm T}.$$

It can be seen that dynamics $p,\ q$ and r can be measured by the IMU, and $\bar{p},\ \bar{q},\ \bar{r}$ can be derived from the outer-loops. Then, the real fast variables can be formulated as $p_{\rm f} = p - \bar{p},\ q_{\rm f} = q - \bar{q},\ r_{\rm f} = r - \bar{r}$.

Denoting a pseudo control

$$v_{\rm f} = \begin{bmatrix} a_2(q_{\rm f}r_{\rm f} + \bar{q}r_{\rm f} + q_{\rm f}\bar{r}) + b_2u_{2\rm f} \\ a_3(p_{\rm f}r_{\rm f} + \bar{p}r_{\rm f} + p_{\rm f}\bar{r}) + b_3u_{3\rm f} \\ a_3(p_{\rm f}q_{\rm f} + \bar{p}q_{\rm f} + p_{\rm f}\bar{q}) + b_4u_{4\rm f} \end{bmatrix},$$

then the equivalent linear fast subsystem in the fast time-scale using the dynamic inversion approach is represented as $\dot{z}_{\rm f} = v_{\rm f}$. We found that the real fast control $u_{\rm ff}$ can be calculated by $u_{\rm ff} = v_{\rm f} - M$, where

$$M = \begin{bmatrix} a_2(q_{\rm f}r_{\rm f} + \bar{q}r_{\rm f} + q_{\rm f}\bar{r}) \\ a_3(p_{\rm f}r_{\rm f} + \bar{p}r_{\rm f} + p_{\rm f}\bar{r}) \\ a_3(p_{\rm f}q_{\rm f} + \bar{p}q_{\rm f} + p_{\rm f}\bar{q}) \end{bmatrix}.$$

Taking $v_{\rm f} = Az_{\rm f} + Bu_{\rm in}$, the pseudo linear inner-loop model can be obtained,

$$\dot{z}_{\rm f} = Az_{\rm f} + Bu_{\rm in}, \tag{9}$$

with

$$B = \begin{bmatrix} b_2 & 0 & 0 \\ 0 & b_3 & 0 \\ 0 & 0 & b_4 \end{bmatrix},\ u_{\rm in} = \begin{bmatrix} u_{2\rm f} \\ u_{3\rm f} \\ u_{4\rm f} \end{bmatrix},$$

where A is the prescribed state-space matrices to represent the open-loop characteristics of the inner-loop model. Note that the pair $(A,\ B)$ must be controllable.

If the matrix A is selected to be diagonal,

$$A = \begin{bmatrix} a_{\rm p} & 0 & 0 \\ 0 & a_{\rm q} & 0 \\ 0 & 0 & a_{\rm r} \end{bmatrix},$$

then system (9) can be decomposed into three individual subsystems:

–p subsystem:

$$\dot{p}_{\rm f} = a_{\rm p}p_{\rm f} + b_1u_{2\rm f}. \tag{10}$$

–q subsystem:

$$\dot{q}_{\rm f} = a_{\rm q}q_{\rm f} + b_2u_{3\rm f}. \tag{11}$$

–r subsystem:

$$\dot{r}_{\rm f} = a_{\rm r}r_{\rm f} + b_3u_{4\rm f}. \tag{12}$$

Combining SPaTSs with dynamic inversion approaches, the closed-loop inner-loop can be seen in Fig.1.

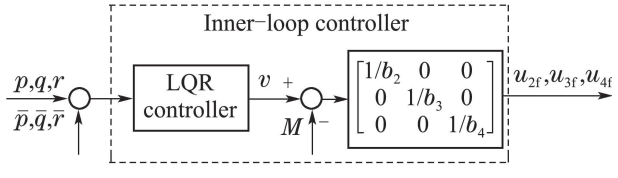

Fig. 1 Inner-loop control structure

LQR is utilized in each inner-loop to ensure good stability margin and strong robustness. It should be pointed out that LQR is an optimal control approach based on closed-loop optimal control with the linear state feedback,

$$\begin{cases} u_{2\rm f}(\tau) = -\kappa_{\rm p}p_{\rm f}(\tau), \\ u_{3\rm f}(\tau) = -\kappa_{\rm q}q_{\rm f}(\tau), \\ u_{4\rm f}(\tau) = -\kappa_{\rm r}r_{\rm f}(\tau), \end{cases}$$

and $k_{\rm p},\ k_{\rm q},\ k_{\rm r}$ are searched, respectively, to minimize the cost function

$$J = \int_0^\infty \{z_{\rm f}(\tau)^{\rm T}Qz_{\rm f}(\tau) + u_{\rm in}^{\rm T}(\tau)Ru_{\rm in}(\tau)\}{\rm d}\tau,$$

with Q a symmetric and semi-positive definite matrix, R a definite positive matrix, and

$$K \triangleq \begin{bmatrix} \kappa_{\rm p} & 0 & 0 \\ 0 & \kappa_{\rm q} & 0 \\ 0 & 0 & \kappa_{\rm r} \end{bmatrix}.$$

The anticipate time-domain characteristics can be achieved by reasonable weight matrix configuration.

Remark 1 The LQR problem can be regarded as minimizing the cost formulated as a linear combination of the states $z_{\rm f}$ and the control input $u_{\rm in}$. The weighting matrix Q is used to tighten the states are to be controlled, and the matrix R weights the amount of control action. Commonly, Q and R are selected as diagonal matrices.

In closed loop, the performance index J can be rewritten as

$$J = \int_0^\infty \{z_{\rm f}(\tau)^{\rm T}(Q - K^{\rm T}RK)z_{\rm f}(\tau)\}{\rm d}\tau.$$

The state feedback gain K can be achieved by $K = R^{-1}B^{\rm T}P$, and P is obtained by solving the algebraic Riccati equation (ARE)

$$A^{\rm T}P + PA - PBR^{-1}B^{\rm T}P + Q = 0. \tag{13}$$

The characteristics of the control system can be investigated with the closed-loop poles. If the transient response specifications or the magnitude constraints are not satisfied, then we resort to re-choosing Q and/or R and repeating the above procedure.

Thus, the nonlinear control law for the inner-loop model (8), formulated by the dynamic inversion approach and LQR technique, is $u_{\rm ff} = -Kz_{\rm f}(\tau) - M$.

Remark 2 The inner-loop controller design method in this paper has advantages compared with other existing methods.

1) Based on the dynamic inversion approach, the three-order inner-loop model can be fully decoupled into three single-input-single-output (SISO) subsystems, and classical control techniques, simple and practical, can be applied hereinafter.

2) It should be noted in [15] that LQR ensures robustness by giving a gain margin of $(-6, \infty)$ db and a phase margin of $(-60, 60)$ degrees, which enhance the robustness of the flight

system. Specific choice of weighing matrices Q and R can give the desired poles.

3) Controller design difficulty caused by the under-actuated nature of MAVs is attenuated. Angular velocities $p,\ q$ and r are separated into two groups, $(p_{\rm s}, q_{\rm s}, r_{\rm s})$ and $(p_{\rm f}, q_{\rm f}, r_{\rm f})$, during the inner-loop controller design procedure. The slow part $(p_{\rm s}, q_{\rm s}, r_{\rm s})$, achieving similar state variation rates as translational dynamics, is selected to be pseudo control input for the outer-loops, and $(p_{\rm f}, q_{\rm f}, r_{\rm f})$, the real fast components, should be stabilized.

3.2 Outer-loop controller design

In this subsection, the outer-loop controller is designed based on the dynamic inversion approach and PID control technique to achieve desired path tracking performance.

To attenuate the controller design difficulty caused by the under-actuated nature of MAVs, the "slow part" of z can be chosen as the pseudo control input of the outer-loop. In [16], it has been noted that the number of control input should be equal to that of states. In this sense, the slow states to be controlled can be selected as $x_{\rm c} = [u\ \ v\ \ w\ \ \phi]^{\rm T}$, and the remaining slow states, $x_{\rm f} = [\theta\ \ \psi]^{\rm T}$, can be treated as free variables.

The controlled subsystem $\Sigma_{\rm c}$ of outer-loop can be written in the following form,

$$\dot{x}_{\rm c} = f_{\rm c}(x_{\rm f}) + f_{\rm u}(x_{\rm c})\bar{u}_{\rm s}, \tag{14}$$

where

$$\begin{cases} f_{\rm c}(x_{\rm f}) = \begin{bmatrix} -{\rm g}s\theta \\ {\rm g}s\phi c\theta \\ {\rm g}c\phi c\theta \\ 0 \end{bmatrix}, \\ f_{\rm u}(x_{\rm c}) = \begin{bmatrix} 0 & -w & v & 0 \\ w & 0 & -u & 0 \\ -v & u & 0 & 1/m \\ 1 & s\phi\tan\theta & c\phi\tan\theta & 0 \end{bmatrix}, \\ \bar{u}_{\rm s} = [p_{\rm s}\ \ q_{\rm s}\ \ r_{\rm s}\ \ u_1]^{\rm T}, \end{cases}$$

and we have

$$u_{\rm fs} = -[a_2 q_{\rm s} r_{\rm s}/b_2\ \ a_3 p_{\rm s} r_{\rm s}/b_3\ \ a_4 q_{\rm s} q_{\rm s}/b_4]^{\rm T}.$$

The uncontrolled subsystem $\Sigma_{\rm f}$ of the slow subsystem can then be formulated as

$$\dot{x}_{\rm f} = f_{\rm f}(x_{\rm f})\bar{u}_{\rm s}, \tag{15}$$

where

$$f_{\rm f}(x_{\rm f}) = \begin{bmatrix} 0 & c\phi & s\phi & 0 \\ 0 & s\phi\sec\theta & c\phi\sec\theta & 0 \end{bmatrix}.$$

Remark 3 It should be remarked that once control strategy is designed for $\Sigma_{\rm c}$ to achieve desired tracking performance, and the movement laws of states θ and ψ can be formulated subsequently based on internal structure. Thereby, the controlled subsystem $\Sigma_{\rm c}$ is the focus hereinafter.

Defining a pseudo control input $v_{\rm s}$, one can derive the equivalent linear model of $\Sigma_{\rm c}$ via the dynamic inversion approach, $\dot{x}_{\rm c} = v_{\rm s}$, where $v_{\rm s} = f_{\rm c}(x_{\rm f}) + f_{\rm u}(x_{\rm c})\bar{u}_{\rm s}$. The real control of the outer-loop can be calculated by $\bar{u}_{\rm s} = f_{\rm u}^{-1}(x_{\rm c})[v_{\rm s} - f_{\rm c}(x_{\rm c})]$. States $x_{\rm c}$ and $x_{\rm f}$ can be measured by a IMU to guarantee the feasibility of the dynamic inversion approach.

Remark 4 The sufficient condition for the existence of the inversion of $f_{\rm u}^{-1}(x_{\rm c})$ is $\det(f_{\rm u}(x_{\rm c})) \neq 0$. For most trajectory tracking cases of UAVs, such condition can be guaranteed. However, x in the last measurement time should be kept when $f_{\rm u}^{-1}(x_{\rm c})$ does not exist.

For given position $\xi_{\rm d}(t)$ and roll angle $\phi_{\rm d}(t)$, the desired slow state can be derived $x_{\rm d}(t) = [\dot{\xi}_{\rm d}(t)\ \ \phi_{\rm d}(t)]^{\rm T}$.

A PID controller, utilized in the outer-loop, is a generic control loop feedback mechanism and regarded as the standard control structures of the classical control theory. To improve the tracking performance, the slow errors can be formed by combination of position errors and velocity errors,

$$x_{\rm e}(t) = [x_{\rm d}(t) - x_{\rm c}(t)] + [\xi_{\rm d}(t) - \xi(t)].$$

Then, the PID control can be derived

$$v_{\rm s} = k_{\rm p} x_{\rm e}(t) + k_{\rm i}\int_0^t x_{\rm e}(t) + k_{\rm d}\frac{{\rm d}x_{\rm e}(t)}{{\rm d}t},$$

where $k_{\rm p},\ k_{\rm i}$ and $k_{\rm d}$ are related PID gains. By adjusting PID gains, the errors can reach zero, and desired tracking performance can be achieved. The closed-loop outer-loop can be shown in Fig.2.

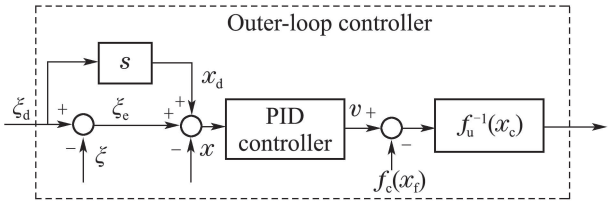

Fig. 2 Outer-loop control structure

Remark 5 PID control, simple and practical, is utilized in the outer-loop controller design, which is sufficient to achieve desired path tracking performance. PID gains, $k_{\rm p},\ k_{\rm i}$ and $k_{\rm d}$ can be determined by trial and error method.

4 Design procedure

Complex future missions in civilian and military scenarios will require UAVs to exploit their full dynamic capabilities. For the trajectory tracking, translational dynamics (slow states) are mainly related with tracking performance. Wind disturbances may cause large initial state errors, and orientation-

al dynamics (fast states) are easily excited by high-frequency wind disturbances. It can be seen that lacking effective control strategy for fast states may lead to instability or poor performance of the flight system.

In this paper, the dual loop control structure is adopted to achieve the desired tracking performance and sufficient stability. The inner-loop controller is composed by a dynamic inversion controller and a LQR controller to achieve considerable stability margin, and two time-scale characteristics can be preserved. The outer-loop controller combines a dynamic inversion controller with a PID controller for significant performance distinctiveness (tracking performance). It can be verified that the dual loop control structure, shown in Fig.3, can simplify the design procedure and improve the control quality, which paves a new way for dealing with high-frequency dynamics.

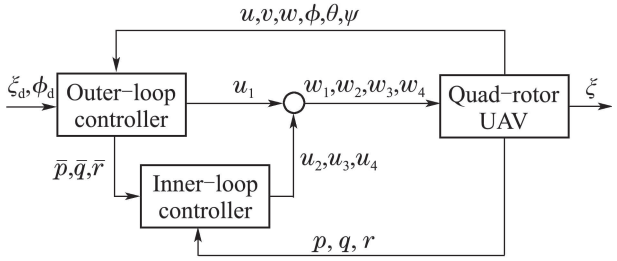

Fig. 3 Dual-loop control structure

The design process is carried out based on the following steps.

Step 1 We establish the singularly perturbed model (4) of a UAV based on first principle or system identification techniques. In this step, parameters of the quad-rotor MAV are obtained, and the small positive scalar ϵ is determined to characterize the two time-scale nature of the flight system.

Step 2 We construct inner-loop and outer-loop models via SPaTSs and dynamic inversion approaches. In this step, the original high-order flight control system has been fully decomposed into reduced subsystems, and controllers for subsystems can be design individually.

Step 3 We design the inner-loop controller. Weighing matrices Q and R are chosen, and the ARE (13) is solved to compute the LQR controller gain K. Check the time response of the inner-loop whether the desired stability requirement is satisfied. If not, reselect Q and R and repeat this step.

Step 4 We obtain the outer-loop controller. Adjust the PID gains constantly to ensure desired trajectory tracking performance.

Step 5 We formulate the composite control, which can be applied to the original MAV control system,

$$\begin{cases} \bar{u}_{\rm s} = f_{\rm u}^{-1}(x_{\rm c})[v_{\rm s} - f_{\rm c}(x_{\rm c})], \\ u_{\rm f} = u_{\rm fs} + u_{\rm ff}, \end{cases} \tag{16}$$

with

$$u_{\rm ff} = v_{\rm f} - M,$$
$$u_{\rm fs} = -[a_2 q_{\rm s} r_{\rm s}/b_2 \quad a_3 p_{\rm s} r_{\rm s}/b_3 \quad a_4 q_{\rm s} q_{\rm s}/b_4]^{\rm T}.$$

Real controls $u_1,\ u_2,\ u_3$ and u_4 can be obtained from $\bar{u}_{\rm s}$ and $u_{\rm f}$.

5 Simulation results

Before the practical implementation, we have carried out a series of Matlab-based simulations to demonstrate the validity of results in trajectory tracking of the quad-rotor MAV. Taking the nonlinear model (1) of quad-rotor MAV as the plant, the entire flight control system is tested in the simulation. Related parameters are listed in Table 2.

Table 2 Parameters of a UAV dynamic model

Parameter	Value
m	$0.5\,\mathrm{kg}$
g	$9.781\,\mathrm{kg\cdot m^{-2}}$
l	$0.2\,\mathrm{m}$
$I_{\rm x}$	$0.114\,\mathrm{kg\cdot m^2}$
$I_{\rm y}$	$0.114\,\mathrm{kg\cdot m^2}$
$I_{\rm z}$	$0.158\,\mathrm{kg\cdot m^2}$

Taking the fast response rate of LQR controller into consideration, it is straightforward that LQR scheme is well suited in the inner-loop to guarantee sufficient stability of the fast states. The related LQR controller gain is chosen as

$$\kappa_{\rm p} = 20,\ \kappa_{\rm q} = 20,\ \kappa_{\rm r} = 20,$$

with $a_{\rm p} = 1,\ a_{\rm q} = 1$ and $a_{\rm r} = 0.3$. In Fig.4, it is shown that the real fast dynamics converge to zero quickly with aid of the LQR controller, which can ensure smooth operation of the whole flight system.

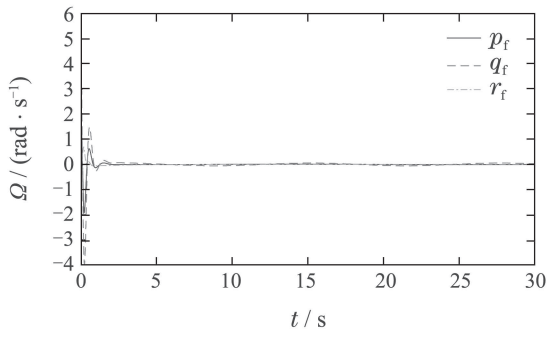

Fig. 4 Inner-loop dynamics

It can be seen from Fig.5 that the translational velocities $u,\ v$ and w achieve good time responses with

respect to step, ramp and acceleration signals. Fig.6 illustrates that the trajectory tracking part of the design procedure works fairly well following the given reference with a high accuracy. One of the reasons for that is that both translational and orientational constraints are carefully considered, and related PID gains are carefully selected and constantly adjusted to wipe out errors caused by wind. In this case, the pqr loop PID gains are chosen as

$$k_{\mathrm{p}} = 20,\ k_{\mathrm{i}} = 8,\ k_{\mathrm{d}} = 1,$$

and the ϕ loop PID gains are selected as

$$k_{\mathrm{p}} = 0.5,\ k_{\mathrm{i}} = 0.05,\ k_{\mathrm{d}} = 0.$$

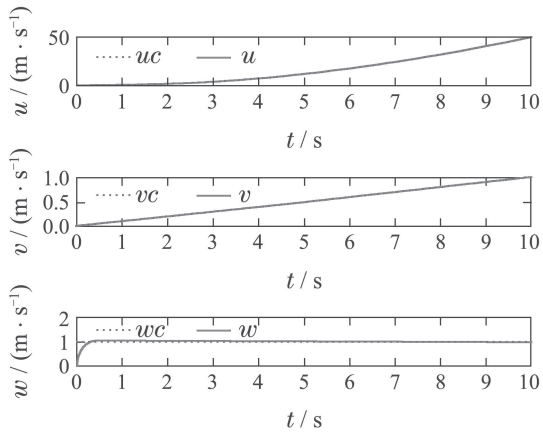

Fig. 5 Time responses of the outer-loop

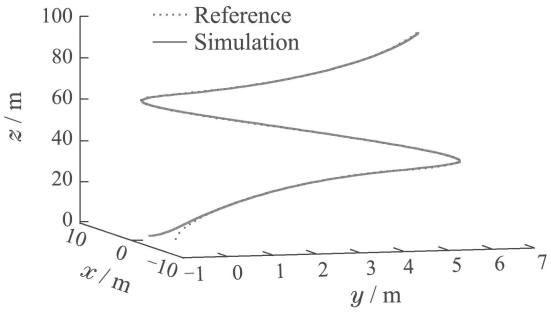

Fig. 6 Tracking performance

In Fig.7, motions of Euler angles are revealed. Once the controlled dynamics u, v, w and ϕ are formed, the remaining free dynamics θ and ψ can be determined. As mentioned, the slow part of the fast state p, q and r is selected as the pseudo control input for outer-loops such that all the translational dynamics can be controlled, and the pseudo control is demonstrated in Fig.8.

Fig.9 reveals the real controls u_1, u_2, u_3 and u_4. The controller gains are not high, and the whole control energy in this flight system is permitted from engineering perspective.

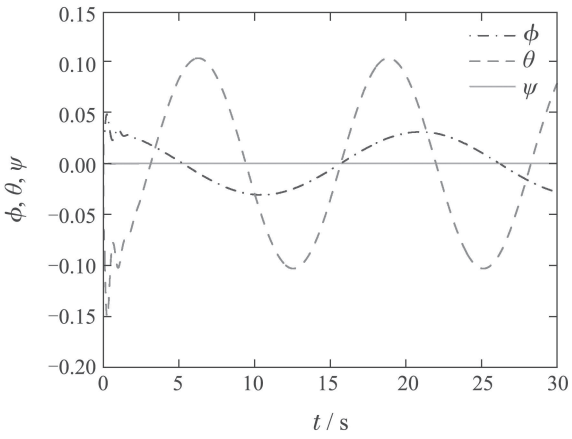

Fig. 7 Euler angles

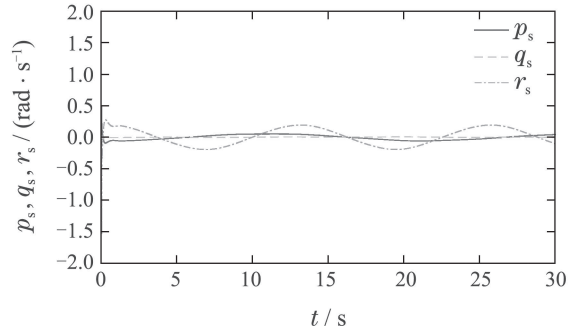

Fig. 8 Pseudo control input

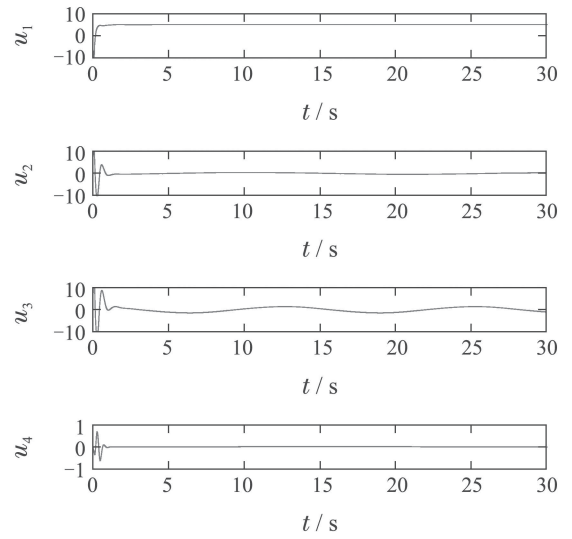

Fig. 9 Control input

Remark 6 Compared with the existing methods, the controller design method of this work exhibits many advantages.

1) Advantage is thereby taken of the singularly perturbed nature of the MAV flight system to design a well-conditioned composite feedback controller to incorporate inner-loop and outer-loop control.

2) Based on the SPaTSs and dynamic inversion approaches, reduced-order SISO subsystems are constructed in different time-scales such that strong coupling between the translational and orientational dy-

namics can be alleviated to reduce the computation complexity.

3) The inner-loop and outer-loop control strategies, LQR and PID control techniques, are simple and practical, which is well-suited for real engineering appliances. Related controller gain can be calculated by MATLAB.

4) The modeling/control approach is ready to be applied in higher level navigation systems for complex autonomous missions.

6 Conclusions

In this paper, a nonlinear path tracking controller is designed for a quad-rotor MAV. The singular perturbed form of a quad-rotor MAV is established to obtain reduced-order subsystems to enhance feasibility of controller design. In order to compensate the damped orientational dynamics, LQR techniques are utilized in inner-loops. For out loops, classical PID control is used to ensure satisfied path tracking performance. To integrate inner-loop control with outer-loop control, the dual-loop control structure is adopted. Simulation results prove the effectiveness of considered approach and demonstrate that the quad-rotor MAV can follow the given path fairly well. Future work will concentrate on extending the developed controller to making the MAV more robust and capable of onboard, real-time implementation.

References:

[1] ABDESSAMEUD A, TAYEBI A. Global trajectory tracking control of VTOL-UAVs without linear velocity measurements [J]. *Automatica*, 2010, 46(6): 1052 – 1059.

[2] AGUIAR A, HESPANHA J. Trajectory-tracking and path-following of underactuated autonomous vehicles with parametric modeling uncertainty [J]. *IEEE Transactions on Automatic Control*, 2007, 52(8): 1362 – 1375.

[3] XU R, OZGUNER U. Sliding mode control of a class of underactuated systems [J]. *Automatica*, 2008, 44(1): 233 – 241.

[4] WENZEL K, MASSELLI A, ZELL A. Automatic take off, tracking and landing of a miniature UAV on a moving carrier vehicle [J]. *Journal of Intelligent & Robotic Systems*, 2001, 61(1): 221 – 238.

[5] LARA D, ROMERO G, SANCHEZ A, et al. Robustness margin for attitude control of a four rotor mini-rotorcraft: case of study [J]. *Mechatronics*, 2010, 20(1): 143 – 152.

[6] 姚远, 周兴社, 张凯龙, 等. 基于稀疏A^*搜索和改进人工势场的无人机动态航迹规划 [J]. 控制理论与应用, 2010, 27(7): 953 – 959.
(YAO Yuan, ZHOU Xingshe, ZHANG Kailong, et al. Dynamic trajectory planning for unmanned aerial vehicle based on sparse A^* search and improved artificial potential field [J]. *Control Theory & Applications*, 2010, 27(7): 953 – 959.)

[7] 辛哲奎, 方勇纯, 张雪波. 小型无人机地面目标跟踪系统机载云台自适应跟踪控制 [J]. 控制理论与应用, 2010, 27(8): 1001 – 1006.
(XIN Zhekui, FANG Yongchun, ZHANG Xuebo, et al. Dynamic trajectory planning for unmanned aerial vehicle based on sparse A^* search and improved artificial potential field [J]. *Control Theory & Applications*, 2010, 27(8): 1001 – 1006.)

[8] WANG L, JIA H. The trajectory tracking problem of quadrotor UAV: Global stability analysis and control design based on the cascade theory [J]. *Asian Journal of Control*, 2014, 16(2): 574 – 588.

[9] ZHANG Y, YANG X, ZHAO H, et al. Tracking control of UAV trajectory [C] //*Proceedings of 2014 IEEE Chinese Guidance, Navigation and Control Conference (CGNCC)*. Yantai: IEEE, 2014: 1889 – 1894.

[10] KOKOTOVIC P, KHALIL H, O'REILLY J. *Singular Perturbation Methods in Control: Analysis and Design* [M]. New York: Academic Press, 1986.

[11] BERTRAND S, GUENARD N, HAMEL T, et al. A hierarchical controller for miniature VTOL UAVs: design and stability analysis using singular perturbation theory [J]. *Control Engineering Practice*, 2011, 19(10): 1099 – 1108.

[12] MENON P, WALKER R. Nonlinear flight test trajectory controllers for aircraft [J]. *Journal of Guidance*, 1987, 10(1): 67 – 72.

[13] SHIAU J, MA D. An autopilot design for the longitudinal dynamics of a low-speed experimental UAV using two-time-scale cascade decomposition [J]. *Transactions of the Canadian Society for Mechanical Engineering*, 2009, 33(3): 501 – 521.

[14] KIM J, KANG M, PARK S. Accurate modeling and robust hovering control for a quad-rotor VTOL aircraft [J]. *Journal of Intelligent and Robotic Systems*, 2010, 57(14): 9 – 26.

[15] LIEBST B. A linear quasratic regulator weight selection algorithm for robust pole assignment [C] //*Proceedings of AIAA Guidance, Navigation and Control*. New Orleans, LA: Aerospace Research Central, 1990: 36 – 45.

[16] FRANCO A, BOURLES H, DE PIERI E, et al. Roubst nonlinear control associating robust feedback linearization and H_∞ control [J]. *IEEE Transactions on Automatic Control*, 2006, 51(7): 1200 – 1207.

作者简介:

许 璟 (1990–), 女, 博士研究生, 主要研究方向为奇异摄动系统、故障检测与诊断、鲁棒控制、UAV飞行控制, E-mail: xujing_paper@sina.com;

蔡晨晓 (1975–), 女, 博士, 教授, 主要研究方向为奇异摄动系统、广义系统、鲁棒控制、UAV飞行控制, E-mail: ccx5281@vip.163.com;

李勇奇 (1992–), 男, 主要研究方向为奇异摄动系统、UAV飞行控制, E-mail: yongqi lee@hotmail.com;

邹 云 (1962–), 男, 教授, 导师, 主要研究方向为奇异系统、多维系统、UAV控制系统、智能电网等, E-mail: zouyun@vip.163.com.